

Stochastic model for subsurface water flow in Swiss catchments

M.C. Bovier^{a,c}, S. Fedotov^b, S. Ferraris^c, A. Gentile^c, B. Toaldo^a

^a Department of Mathematics “Giuseppe Peano”, University of Turin, Torino, Italy

^b Department of Mathematics, The University of Manchester, Manchester, UK

^c Interuniversity Department of Regional and Urban Studies and Planning (DIST), Polytechnic and University of Turin, Torino, Italy

ARTICLE INFO

Keywords:

Heterogeneous catchments
Subsurface flow
Stable water isotopes
Young water fraction
Transit time
Stochastic model

ABSTRACT

Understanding water movement in catchments subsurface is crucial for numerous applications such as pollutant contamination, nutrient loss, water resource management and ecosystem functioning. Among the variables of particular interest, the transit times of water particles and their statistical distribution are a desirable output. Nevertheless, past approaches assume explicitly the form of the transit time distribution (TTD) to provide information on water age in catchments. In this study we adopt a different approach by making assumptions on the movement of water particles in the subsurface instead of assumptions on the transit time distribution. Hence we propose a model based on a random velocity process with rests, where a water particle alternatively moves with a constant velocity or it is trapped (with zero velocity) until it reaches the outlet of the catchment. We assume that the moving times are i.i.d. (independent and identically distributed) random variables with exponential distribution, while waiting times, i.e., times in which the water particle is trapped in subsurface cavities, are assumed to be i.i.d. random variables with Mittag-Leffler distribution of order α , which is heavy tailed. At the catchment outlet, which is assumed here to be at a distance from the inlet equal to the catchment median flow path length L , the first passage time (or transit time) of the water particles is measured.

We applied the model to 22 Swiss catchments simulating, for each catchment, the movement of millions of water particles thus obtaining the corresponding empirical TTD. We search for the threshold age (τ^*) that closely approximates the portion of the empirical TTD younger than τ^* , that is the young water fraction (F_{yw}). We use the complex modulus of the empirical characteristic function of the TTD: this quantity represents, in our model, the amplitude ratio of seasonal isotope cycles in stream water and precipitation. Our results reveal that τ^* is comprised between 46 and 76 days, exactly in the range 2-3 months previously identified. Additionally, given the amplitude ratio of isotopic concentrations, we estimate the only parameter of the model, that is the α parameter of the Mittag-Leffler distribution, for each Swiss catchment using suitable catchments properties. In conclusion, our study reveals that random velocity processes with rests are stochastic transport processes useful for modeling water movement in heterogeneous catchments, with a limited number of assumptions.

1. Introduction

The transit time of water can be defined as the elapsed time from the input of the water through the catchment inlet at time t_{in} to the output of the water through the catchment outlet at time t_{out} (Rigon et al., 2016). Accordingly, the transit time is the time that it takes for rainfall (or snowmelt) to travel through a catchment before being released as streamflow (Kirchner, 2016a). The transit time of water, and thus the water age, is an important catchment descriptor that gives information on flow paths which controls solutes transport which in turn influences the susceptibility to pollutant contamination and nutrient loss (McGuire and McDonnell, 2006; Benettin et al., 2022; Porporato and Calabrese, 2015).

Porporato and Calabrese (2015) examined existing theories of age distributions in hydrologic systems and highlighted the need to treat these distributions as random functions when fluxes are modeled with time-varying stochastic processes. They used a stochastic model to illustrate how the probabilistic structure of age distributions can help quantify the variability and inherent uncertainty in determining water age in real systems. Subsequently, Calabrese and Porporato (2017) analyzed the role of multiple outflows, spatial components, and nonlinearities in the age theory. The water age and the movement of dissolved substances are closely interconnected and are frequently investigated in conjunction (Benettin et al., 2017). In the framework of stochastic models, continuous time random walk (CTRW) models were typically used in studies of chemical transport. For example, a recent study

* Corresponding author.

E-mail address: mariachiara.bovier@unito.it (M.C. Bovier).

of Dentz et al. (2023) has investigated the occurrence of anomalous (non-Fickian) transport of chloride in a catchment system over a multi-decadal period. Moreover, Goeppert et al. (2020), by investigating the tracer breakthrough curves in a karst system at the border between Germany and Austria, found that CTRW better describes the low concentrations at longer travel times rather than traditional advection–dispersion model and the two-region non-equilibrium model. However, efforts are beginning to adapt these CTRW models also for the movement of water particles. In this regard, in a very recent study, Elhanati et al. (2024) implemented a continuous time random walk-particle tracking (CTRW-PT) numerical model to quantify long-tailed breakthrough curves in a karst system of the Austrian Alps, drawing an analogy between partially saturated karst flow and chemical transport.

Past (pre-2006) methodologies that aimed to estimate the mean transit time (MTT) relied on an assumed time-invariant transit time distributions (e.g., general steady-state lumped convolution or flow weighted time) (Benettin et al., 2022). However, the importance and interest in unraveling the mechanisms by which watersheds retain water, sometimes for years, before releasing it in a matter of hours (Kirchner, 2003) have led to significant developments in the field of transit time estimation by using new data, theory and applications (Benettin et al., 2022). From the experimental point of view stable water isotopes have been used and are increasingly being used in catchment hydrology to investigate the *velocity* of the water molecules and, thus, the water transit time (Kendall and McDonnell, 1998). Among the cutting-edge theories that use such data, one that has gained significant traction is based on the use of (time-invariant or time-variant) StorAge Selection (SAS) function (Botter et al., 2011), which quantifies the release of waters of different ages from the storage to an outflow (Rinaldo et al., 2015).

Nevertheless, additional data-based methodologies have been developed in recent years. The pre-2006 methods have been questioned since they implicitly assume homogeneous and stationary catchments with consequent underestimation of the MTTs (Kirchner, 2016a,b). As a result, it has been necessary to find a new metric, different from the MTT, that is not sensitive to spatial heterogeneity and hydrologic non-stationarity and that is able to infer reliable information directly from seasonal tracer cycles. In this regard, Kirchner (2016a) and Kirchner (2016b), assuming that the TTD belongs to the family of gamma distributions in thought experiments of mixing runoff, revealed that the ratio of the amplitudes of seasonal isotope cycles in streamflow and precipitation, respectively, is unaffected by the so-called aggregation bias and that this ratio quantifies the fraction of runoff with transit times younger than a threshold age of 2–3 months, named young water fraction (F_{yw}) (Kirchner, 2016a,b).

The gamma distribution has been chosen by Kirchner (2016a) for mathematical convenience: it is conveniently parameterized and it possesses finite moments of all orders and thus the family of gamma distributions encompasses a wide range of shapes which approximate many plausible TTDs. Furthermore, merging subcatchments runoff (with assumed gamma TTD), the resulting runoff reveals a non-gamma TTD, thus suggesting a general validity of his results (Kirchner, 2016a). Nevertheless, the a-priori choice of the TTD is a limitation since it is an assumption on a desired output. Indeed, other robust methods have been developed to infer the transit time distribution such as non-parametric deconvolution methods (Cirpka et al., 2007; Payn et al., 2008; Gooseff et al., 2011). These approaches have been particularly useful, for example, to determine transit time distributions using electrical conductivity time series or to derive stream solute residence time distributions from natural tracer concentrations without presuming any shape of the distribution. Also, other simple assumptions would lead to an exponential TTD (e.g., Benson et al. (2019)).

Taking a step back, the TTD can be seen as the observed effect at the outlet point concerning the movement of water particles within the watershed. Accordingly, what is reasonable to be assumed is the

movement of water molecules in the subsurface. To investigate groundwater dynamics, a variety of numerical modeling approaches, based on Darcy's Law, have been used and constrained on different field data (Somers and McKenzie, 2020). Such data can be estimated from boreholes in the plains, while they are scarce for mountain environments in which subsurface processes are largely unknown. Thus, the reproduction of observations as a result of hydrological processes at catchment-scale remains challenging due to largely unknown boundary conditions (Somers and McKenzie, 2020). Stochastic models, even if they are based on approximations about the physics of the process, can partially include the complex phenomena occurring in the subsurface with simple assumptions that overcome a detailed knowledge of boundary and initial conditions and result suitable for practical applications.

The concept of first passage time refers to quantifying the time taken by a random quantity to reach a preset threshold value. Therefore, the theory of first passage times is well-suited for describing the movement of a water molecule within a catchment until it reaches the outlet point. A past theoretical study of Godoc and Metzler (2016) advanced the first passage theory by rigorously deriving the complete distribution of first passage times for a heterogeneous system (like catchments are) and by uncovering significant differences between typical first passage times and mean first passage times. However, studies that utilize the first-passage time theory in hydrological studies with experimental data capable of validating the model outputs are still limited.

Another modeling approach, which is widely used for anomalous transport in heterogeneous systems, is the mobile-immobile (MIM) model, which separates the particles into two fractions, those that are in the mobile zone and those that are trapped in the immobile zone. The convectional (Markovian) MIM model was used by Gao et al. (2010) to describe reactive solute transport with scale-dependent dispersion in heterogeneous porous media by assuming the dispersivity coefficient a linear or exponential function of travel distance. Instead a fractional mobile-immobile model for solute transport was considered, for example, by Schumer et al. (2003) or Benson and Meerschaert (2009). Assuming the power law distribution for waiting times in the immobile zone leads to a fractional time derivative in the model equations. The solutions capture the anomalous behavior of tracer plumes in heterogeneous aquifers, including power law breakthrough curves at late time, and power law decline in the measured mobile mass. Mobile-immobile models with power-law and mixed waiting time distributions was considered also by Doerries et al. (2022). They studied different forms for the dynamics of trapping times, not restricted to the exponential, and their effects on tracer mass in the mobile zone, in particular they also considered Mittag-Leffler trapping time distribution. Non-markovian mobile-immobile models are not only used in the geophysical and hydrological contexts. Indeed Kurilovich et al. (2022) developed a non-Markovian MIM model that describes the anomalous subdiffusive behavior of excitons in two different classes of materials. Theoretical and simulated models based on the idea that the trapping time distribution has power-law asymptotics at long times fit the available experimental data.

The main aim of this paper is to develop a novel stochastic model, based on random velocity processes with rests, making plausible assumptions (that take into account the heterogeneity of the catchments subsurface) on distributions of water particles moving times (i.e., the times in which water particles move in the catchment subsurface) and waiting times (i.e., the times in which the water particles are trapped in the catchment subsurface) and validate the model by using results obtained with stable water isotopes across 22 study catchments in Switzerland. The strength of our model is the absence of a-priori assumptions on the TTD, the simplicity of the underlying assumptions on water movement and the requirement of only one input, i.e., the median flow path length L of the catchment, which can be easily obtainable from digital elevation models (DEM) and that will be used as the preset threshold value for calculating the first passage time. It

is noteworthy that this parameter was already found to be strongly correlated with MTTs and F_{yw} in previous studies (McGuire et al., 2005; Tetzlaff et al., 2009; Seeger and Weiler, 2014; von Freyberg et al., 2018).

2. Preliminaries: seasonal cycles of stable isotopes

Isotope seasonal cycle in stream flow can be modeled as the convolution of the catchment's transit time distribution with the isotope seasonal cycle in precipitation (Kirchner, 2016a; McGuire and McDonnell, 2006):

$$c_s(t) = \int_0^{\infty} h(\tau)c_p(t-\tau)d\tau \quad (1)$$

where $c_s(t)$ is the isotopic composition (expressed in delta notation (‰), e.g. $\delta^{18}O$ or δ^2H), in stream flow at time t , $c_p(t-\tau)$ is the isotopic composition in precipitation at any previous time $t-\tau$, and $h(\tau)$ is the transit time distribution T that is a priori unknown. Eq. (1) implicitly assumes that the catchment is a linear time-invariant system and, thus, that the distribution $h(\tau)$ is stationary, i.e., constant in time. Additionally, in this equation the evapotranspiration and its effects on tracer signatures are ignored (Kirchner, 2016a).

The isotopic composition of both stream flow and precipitation follows a seasonal pattern that can be modeled by assuming a sinusoidal function:

$$c_p(t) = A_p \sin(2\pi ft - \phi_p) + k_p, \quad (2)$$

$$c_s(t) = A_s \sin(2\pi ft - \phi_s) + k_s, \quad (3)$$

where A represents the amplitude (‰), ϕ is the phase (radians), t is the time (days), f is the frequency ($f = \frac{1}{365}$ days⁻¹) and k is the constant describing the vertical offset of the isotope signal (‰). The subscripts p and s refers to precipitation and stream flow, respectively. The isotope seasonal cycle of the stream water (i.e., the measured output) exhibits some damping relative to the isotope seasonal cycle of precipitation (i.e., the measured input) and this damping is related to the water age (McGuire and McDonnell, 2006; Kirchner, 2016a). Indeed, the stronger attenuation of the seasonal isotope cycle amplitude in stream flow (A_s) relative to the seasonal isotope cycle amplitude in precipitation (A_p) reflects the longer time that the incoming water spends within the catchment by following complex flow-paths and simultaneously mixing with the groundwater storage which acts as a filter on the input isotopic composition. Accordingly, a lower amplitude ratio (i.e., A_s/A_p) corresponds to older water in the stream.

The amplitude ratio is related to the characteristic function of the transit time distribution as follows. We use \mathbb{E} to denote the mathematical expectation and $H(\xi)$, $\xi \in \mathbb{R}$, for the characteristic function with argument $2\pi\xi$ of $h(\tau)$, hence

$$H(\xi) = \int_{-\infty}^{+\infty} h(\tau)e^{i2\pi\xi\tau}d\tau = \mathbb{E}e^{i2\pi\xi T}. \quad (4)$$

From the convolution (1) and using (2) and (3), it can be obtained that

$$\frac{A_s}{A_p} = |H(f)| \quad (5)$$

where the absolute value of the characteristic function is meant as the complex modulus and f is the frequency of sine functions. For mathematical details see Appendix A.1.

This equivalence between the amplitude ratio of isotope cycles in stream flow and precipitation and the complex modulus of the characteristic function is a key point because A_s/A_p can be quantified by sine-wave fitting on isotope data, while $|H(f)|$ can be computed empirically with simulations. We make assumptions about water movement in the catchment, considering a model based on a random velocity process, and calculate the modulus of the empirical characteristic function of the transit time distribution by simulating the first passage times through a certain level L , as explained in the next section.

3. Mathematical model and methodology

3.1. Random velocity process with rests and passage time

Random velocity processes are transport processes where a moving particle perform random displacements with finite (constant) velocity: random quantities in the model are the length and the orientation of the displacements. In this sense they are a modification of continuous time random walks, which instead are jumping processes (Metzler and Klafter, 2000), and they are very useful to describe a wide range of physical and biological phenomena involving stochastic transport phenomena, since they have continuous trajectories. Furthermore, they can represent different (anomalous) diffusive behavior (Zaburdaev et al., 2015) depending on the tail of the distribution of the displacement's length.

In particular, we consider here a random velocity process with rests, say $X(t)$, $t \geq 0$, for the motion of water particles in the catchment as follows. The particle starts from the origin and moves along a linear path with a constant random velocity v_1 , which is chosen uniformly in the interval $(1, 100)$, for an exponential random time E_1 . Then the particle is trapped and it does not move for a random waiting time J_1 with infinite expectation. At the end of the trapping the motion starts again with another constant velocity v_2 , uniform in $(1, 100)$, for another exponential time E_2 , and so on. It will be always assumed that all the random quantities involved are independent. So the water's particle alternates between moving times, E_n , $n \in \mathbb{N}$, in which it moves with a certain velocity v_n , $n \in \mathbb{N}$, and waiting times (pauses), J_n , $n \in \mathbb{N}$, during which it remains stuck in its current position and thus has zero velocity. The random displacement of the particle represent the motion of the water in the catchment, while the pauses represent some trapping effect induced by catchments' heterogeneity. We remark that random velocity processes can be viewed as semi-Markov models of transporting particle in one dimension, in the sense of Ricciuti and Toaldo (2023), and we use this approach to make the model rigorous, see Appendix A.2 for a precise mathematical formulation.

The assumption on the distribution of the velocities of water particles means that, when particle is free to move, it spreads with velocities v_n , $n \in \mathbb{N}$, that are i.i.d. (independent and identically distributed) random variables with uniform distribution

$$v_n \sim U(1, 100)$$

where the numbers represent a minimum velocity of 1 meters/day and a maximum velocity of 100 meters/day. This is a typical range of seepage velocity, indicated by Devlin (2020), along different types of materials (sandy, sand and gravel, fractured rock, karst).

We choose the exponential distribution with parameter $\lambda = 1$ for moving times since it has finite mean and variance. The choice of the parameter equal to one is justified as follows. An exponential random variable with parameter $\lambda > 0$ is the rescaling of an exponential random variable with parameter 1: if E^λ denote an exponential r.v. with parameter $\lambda > 0$, then $P(E^\lambda/\lambda > t) = P(E^\lambda > t)$. The moving distances traveled by the particles are $E_1^1 v_1, \dots, E_n^1 v_n$, where v_n are the (random) velocities and E_n^1 are i.i.d. copies of E^1 . The rescaling $E_n^\lambda = E_n^1/\lambda$ would be, in practice, nothing more than a deterministic rescaling of the velocities. These, however, must be kept as they are following the discussion above.

Instead, we assume that waiting times are i.i.d. random variables with Mittag-Leffler distribution of order α . The cumulative distribution function is given by:

$$F(t) = P(J_n \leq t) = 1 - E_\alpha(-t^\alpha)$$

where $E_\alpha(\cdot)$ denotes the Mittag-Leffler function of one parameter which is defined as

$$E_\alpha(z) = \sum_{k=0}^{\infty} \frac{z^k}{\Gamma(1 + \alpha k)}.$$

The one-parameter Mittag-Leffler function is a generalization of the exponential function which is very popular in the mathematical community working on non-local equations (see, e.g., Mainardi (2010) and Scalas (2006)). This is because, in particular, the survival function $E_\alpha(-t)$ is the eigenfunction of the fractional derivative of order α , i.e., $\partial_t^\alpha E_\alpha(-t) = -E_\alpha(-t)$ and it reduces to the exponential in the case $\alpha = 1$. For $\alpha \in (0, 1]$ the function $E_\alpha(-t)$ is completely monotone and it is 1 for $t = 0$, this means that is a legitimate survival function. For $\alpha \in (0, 1)$, the function $E_\alpha(-t)$ behaves, see Baleanu et al. (2016), as a stretched exponential for $t \rightarrow 0$

$$E_\alpha(-t) \simeq 1 - \frac{t}{\Gamma(\alpha + 1)} \simeq e^{-\frac{t}{\Gamma(\alpha + 1)}} \quad (6)$$

and has a power law tails for $t \rightarrow \infty$

$$E_\alpha(-t) \simeq \frac{\sin(\alpha\pi) \Gamma(\alpha)}{\pi t} \quad (7)$$

Since $\alpha \in (0, 1)$ the Mittag-Leffler distribution is a heavy tailed distribution (see more on fractional calculus and the corresponding heavy-tailed distributions in Meerschaert and Sikorskii (2012); see Meerschaert and Toaldo (2019) for recent generalizations). The distribution function is differentiable on $(0, +\infty)$ and the density is singular at zero. The behavior of the survival function makes clear that it has infinite mean. We choose the Mittag-Leffler distribution to model the behavior of a water particle subject to a trapping effect in the geological formation of the catchment. Due to the behavior of the Mittag-Leffler distribution the traps tend to be very short, as the density is singular at zero (see Eq. (6)), or very long, as it is an heavy tailed distribution with infinite expectation (see Eq. (7)). The parameter α of the Mittag-Leffler distribution is related to the duration of waiting times, for small α the waiting times are very long while for larger α the waiting times decrease.

In this context the transit time of water in the catchment is represented by the first passage time of the process $X(t)$, $t \geq 0$, through the level L . We choose as level L the median flow path of the catchment because it is a measure for the length of the typical travel of water trajectories in the catchment.

3.2. Computational methods

In order to generate the transit time T_1, \dots, T_N we perform N exact simulations of the trajectories of the process $X(t)$, for t large enough such that all of them pass through the level L (recall that $X(t)$ is continuous and non-decreasing). The simulation are exact in the sense that we can sample all the random quantities from their distribution and then using them to build the trajectories. Given the trajectories, the first passage time is then a functional that we can compute explicitly, see Fig. 1. We generate the water particle velocities as i.i.d. random variables uniformly distributed in the interval $(1, 100)$, the moving times as i.i.d. random variables with exponential distribution with parameter $\lambda = 1$, and the waiting times as i.i.d. random variables with Mittag-Leffler distribution with parameter $0.05 < \alpha < 0.95$ (the extreme values are excluded as they do not appear in our estimates and they are computationally very expensive). The interval $(1, 100)$ meters/day for particle velocities is a typical range of seepage velocity along different types of materials (Devlin, 2020). From the velocities v_n , alternating with zero velocity, we obtain the position of the water particle in time and compute the first passage time for the level L , which corresponds to the measure of the median flow path length in the catchment. The number of iterations has to be sufficiently large for the strong law of large numbers, so we consider $N = 10000$.

Since the distribution function of transit time is unknown, the empirical cumulative distribution function can be computed by simulating N first passage times of a particle for the level L . The empirical characteristic function with N simulated first passage times t_n , $n = 1, \dots, N$ is

$$\overline{H}_N = \frac{1}{N} \sum_{n=1}^N \cos(2\pi f t_n) + i \frac{1}{N} \sum_{n=1}^N \sin(2\pi f t_n). \quad (8)$$

Therefore the complex modulus of the empirical characteristic function is

$$|\overline{H}_N| = \sqrt{\frac{1}{N^2} \left(\sum_{n=1}^N \cos(2\pi f t_n) \right)^2 + \frac{1}{N^2} \left(\sum_{n=1}^N \sin(2\pi f t_n) \right)^2}. \quad (9)$$

The modulus depends on the parameter $\alpha \in (0, 1)$ of the Mittag-Leffler distribution and on the number of simulations N . Since the first passage times t_n are realizations of r.v.'s T_1, \dots, T_N that are i.i.d. copies of T , i.e., the transit time through L of the process, we have by the strong law of large numbers that, almost surely, for $N \rightarrow \infty$,

$$\frac{1}{N} \sum_{n=1}^N \cos(2\pi f T_n) \rightarrow \mathbb{E} \cos(2\pi f T), \quad (10)$$

$$\frac{1}{N} \sum_{n=1}^N \sin(2\pi f T_n) \rightarrow \mathbb{E} \sin(2\pi f T). \quad (11)$$

From (10) and (11) follows that for $N \rightarrow \infty$

$$\begin{aligned} & \sqrt{\frac{1}{N^2} \left(\sum_{n=1}^N \cos(2\pi f T_n) \right)^2 + \frac{1}{N^2} \left(\sum_{n=1}^N \sin(2\pi f T_n) \right)^2} \\ & \rightarrow \sqrt{(\mathbb{E} \cos(2\pi f T))^2 + (\mathbb{E} \sin(2\pi f T))^2}. \end{aligned} \quad (12)$$

Therefore, when the number of simulated first passage times tends to infinity, the modulus of empirical characteristic function tends to the modulus of the theoretical characteristic function, i.e., almost surely as $N \rightarrow +\infty$,

$$|\overline{H}_N| \rightarrow |H(f)|. \quad (13)$$

With N simulated first passage times, given the length of the flow path, we can calculate the modulus of the empirical characteristic function as α varies in $(0, 1)$, using (9). Fig. 2 shows the modulus of the empirical characteristic function computed with different flow path lengths, for α varying.

Therefore, given the median flow path length L of the catchment as a fixed observed parameter, we do the following:

- we obtain N simulated realizations $\underline{t} = (t_1, \dots, t_N)$ of the transit time T of water particles to estimate the empirical TTD, by reaching L ;
- we use that, in our model, the amplitude ratio of the isotopic concentrations is represented by the (complex) absolute value of the TTD characteristic function (see Eq. (5)), that we can estimate empirically through simulations;
- we find, for each catchment, the threshold age τ^* for which the modulus of the empirical characteristic function closely approximates the young water fraction as the model parameter varies (see Section 4.2);
- we show that these threshold ages τ^* agree with the ones obtained by Gentile et al. (2023) and are in the range obtained by Kirchner (2016a) (assuming a gamma TTD). This concludes the validation of the model in the sense proposed by Kirchner (2016a), i.e., our model captures (regardless of the α value) the interplay between the young water fraction and the modulus of the characteristic function;
- we provide an estimate of the model's parameter α which requires the knowledge only of the amplitude ratio (see Section 4.4) and discuss how this parameter is related to the amplitude ratio and the median flow path length.

4. Catchments application and results

4.1. Study catchments

In this study we use the amplitude ratio (A_s/A_p) previously estimated by Gentile et al. (2023) for 22 Swiss catchments (see Fig. 3)

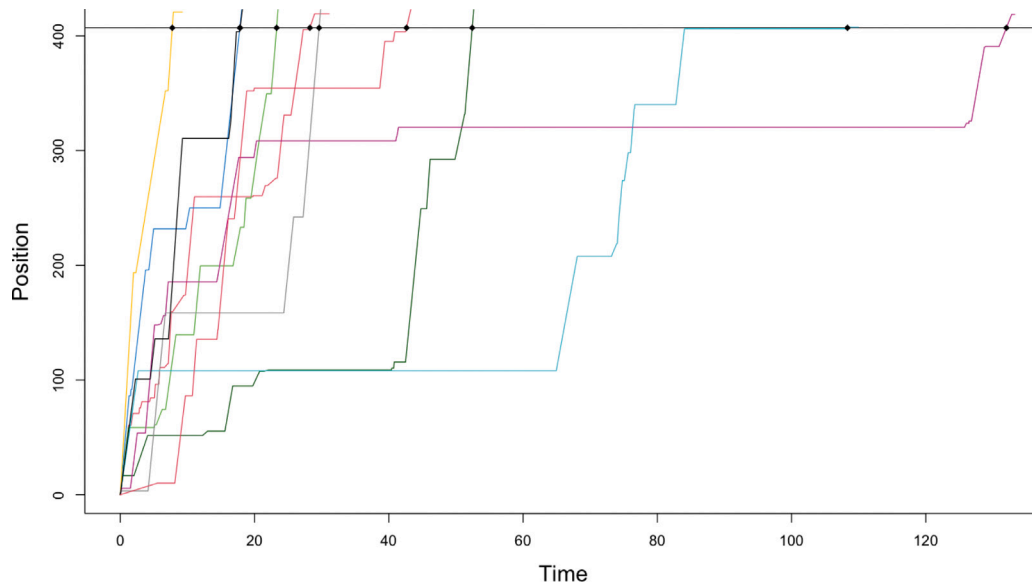


Fig. 1. Simulated trajectories of a water particle through time with first passage times for the level $L = 407$ m.

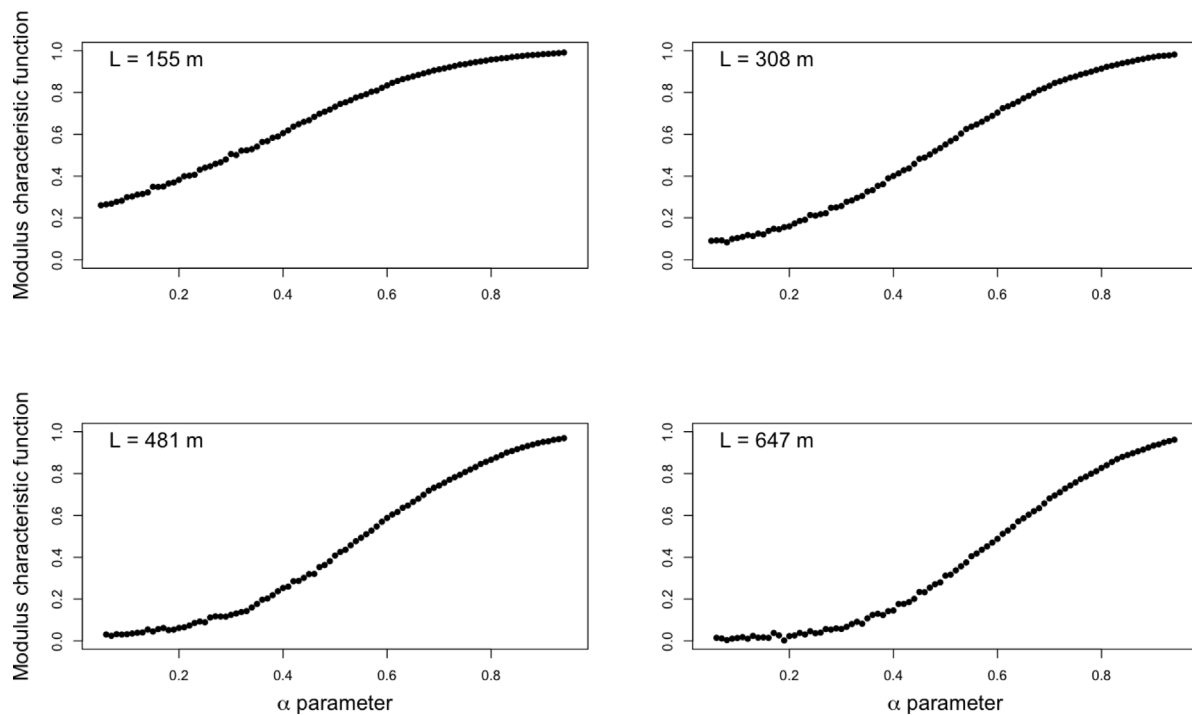


Fig. 2. Modulus of the empirical characteristic function with median flow path lengths: $L = 155$ m, $L = 308$ m, $L = 481$ m and $L = 647$ m, as α varies in $(0,1)$.

which were also investigated by von Freyberg et al. (2018). The amplitudes of seasonal isotope cycles in precipitation and stream flow were obtained in their study by using the isotopic composition ($\delta^{18}O$), complemented with MeteoSwiss daily precipitation data and discharge data. Specifically, the seasonal isotope cycle amplitude in precipitation (A_p) is obtained by fitting volume-weighted Eq. (2) on precipitation isotope data to reduce the influence of low-precipitation periods and to account for temporally aggregated rainfall samples (von Freyberg et al., 2018); the seasonal isotope cycle amplitude in streamwater (A_s) is obtained by fitting flow-weighted Eq. (3) on streamwater isotope data to compensate for sub-sampled high-flow periods. These coefficients are estimated with sinusoidal fitting by using the iteratively re-weighted least squares (IRLS) regression for reducing the influence of outliers. The reader is referred to the source paper (Gentile et al., 2023) for

further information about the methodology and data used to compute the amplitudes of the seasonal cycles which are used in this study to estimate the main parameter of the mathematical model. The amplitude ratios obtained by Gentile et al. (2023) for the 22 Swiss catchments with related standard error (SE) are reported in Table 1. The data set covers catchment mean elevations between 472 and 2369 m a.s.l. and catchment areas between 0.7 and 351 km². The catchments are classified in three different hydro-climatic regimes (snow-dominated, rainfall-dominated and hybrid) according to the classification scheme proposed by Staudinger et al. (2017).

We use as only input data of the mathematical model a terrain index: the median flow path length L (in meters). In this study L is considered as a representative length of the flow paths within the catchment since (i) no more detailed information about the length

Table 1

Name with ID, median flow path length (L), amplitude ratio (A_s/A_p) of isotope cycles in stream flow and precipitation with standard error, threshold age (τ^*) obtained for the young water fraction and estimation of α parameter for the 22 Swiss catchments.

Catchment name (ID)	Median flow path length L (m)	$\frac{A_s}{A_p} \pm SE$	Threshold age τ^* (d)	Parameter estimation $\hat{\alpha}$
Aabach (AAB)	407	0.22 ± 0.04	62	0.35
Aach (AAC)	481	0.07 ± 0.07	66	0.19
Allenbach (ALL)	423	0.14 ± 0.02	63	0.26
Alp (ALP)	196	0.34 ± 0.04	49	0.23
Biber (BIB)	207	0.34 ± 0.04	50	0.25
Dischmabach (DIS)	647	0.09 ± 0.01	76	0.31
Emme (EMM)	286	0.34 ± 0.05	55	0.35
Ergolz (ERG)	421	0.11 ± 0.01	63	0.22
Erlenbach (ERL)	169	0.51 ± 0.05	47	0.35
Guerbe (GUE)	258	0.21 ± 0.03	53	0.18
Ilfis (ILF)	157	0.13 ± 0.02	47	0.006
Langeten (LAN)	308	0.09 ± 0.02	56	0.08
Luempfenbach (LUE)	155	0.33 ± 0.03	46	0.14
Mentue (MEN)	364	0.26 ± 0.05	60	0.35
Murg (MUR)	219	0.11 ± 0.03	50	0.002
Ova da Cluozza (OVA)	616	0.13 ± 0.02	75	0.36
Riale di Calneggia (RIA)	647	0.19 ± 0.03	76	0.44
Rietholzabach (RIE)	194	0.15 ± 0.02	49	0.01
Schaechen (SCH)	646	0.12 ± 0.02	76	0.36
Sense (SEN)	227	0.20 ± 0.04	51	0.13
Sitter (SIT)	329	0.17 ± 0.02	57	0.22
Volgelbach (VOG)	193	0.29 ± 0.03	49	0.17

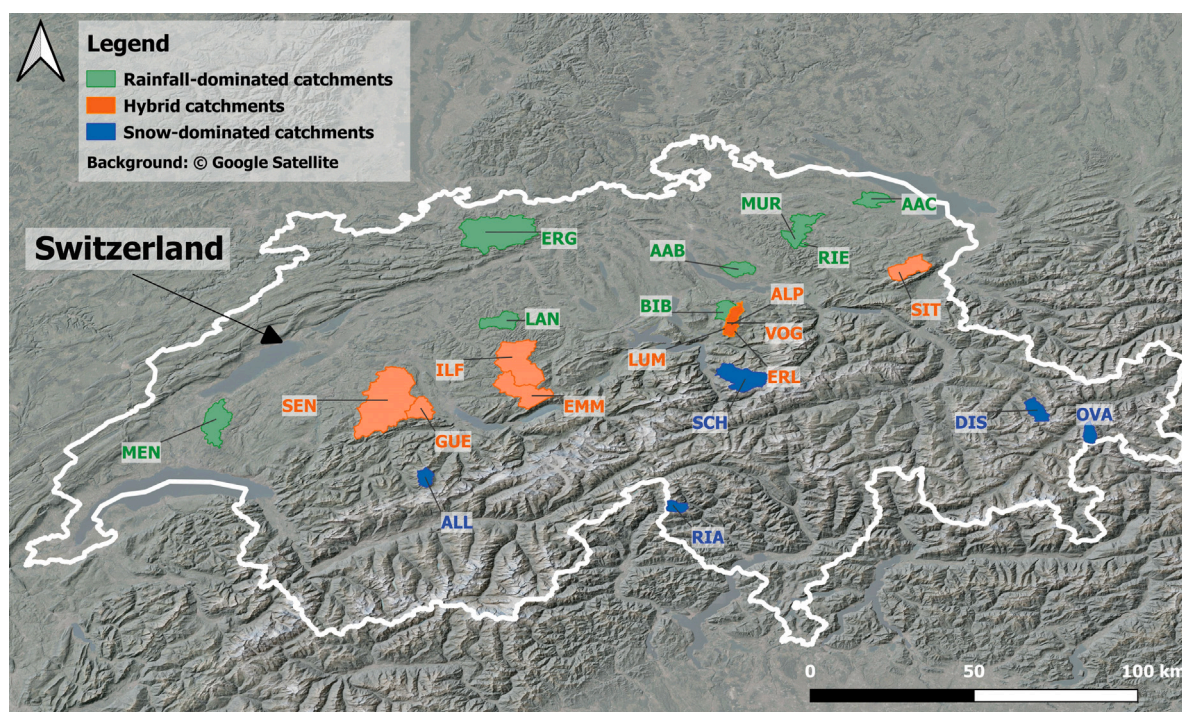


Fig. 3. Location of the 22 study catchments across Switzerland with indication of the hydro-climatic regime.

of subsurface flow paths are available and (ii) it resulted in a strong negative correlation with the young water fraction (von Freyberg et al., 2018), thus it turned out to be a good proxy for the water age. The median flow path lengths reported in Table 1 have been previously computed by Seeger and Weiler (2014) (and reported in Table 2 of von Freyberg et al. (2018)) by using the open source software SAGA-GIS. They used a DEM of 25 m resolution as input to the SAGA module “Channel Network” to derive the channel network in a catchment. Subsequently, they used the SAGA module “Overland Flow Distance to Channel network” (O’Callaghan and Mark, 1984; Freeman, 1991; Ali and De Boer, 2010; Nobre et al., 2011) to calculate the flow path lengths, then aggregated by computing their median value.

4.2. Young water fraction

The young water fraction is defined as the proportion of water younger than a certain threshold age (τ_{yw}) and thus it can be computed using the TTD. Hence, from the point of view of the model, the water younger than a certain τ_{yw} is represented by the distribution function of the TTD, i.e., $P(\tau \leq \tau_{yw})$. This quantity has recently been proposed as a reliable measure of water age in heterogeneous and non-stationary catchments (Kirchner, 2016a,b). Young water fraction with a threshold age of approximately 2–3 months can be estimated directly from the amplitude ratio of the seasonal cycles of stable water isotopes in stream flow and precipitation, respectively (Kirchner, 2016a).

In this section we show that our model, regardless of α and L , captures the behavior of the young water fraction in the sense proposed by Kirchner (2016a). Indeed, the amplitude ratio is represented in our model by the complex modulus of the characteristic function; we show here that this coincides (regardless of α value and for each median flow path) with the proportion of particles that cross level L in less than 2 or 3 months. However, Kirchner (2016a) assumed a Gamma TTD, while we only make hypothesis about the movement of water particles. We can obtain the young water fraction empirically with N simulated first passage times t_n for $\alpha \in (0, 1)$. Denote by

$$(0, +\infty) \ni \tau_{yw} \mapsto F_{yw} = \frac{1}{N} \sum_{n=1}^N \mathbb{1}_{(t_n < \tau_{yw})}. \quad (14)$$

the empirical c.d.f. of the TTD, i.e., the empirical estimate of the fraction of water younger than some arbitrary τ_{yw} , $P(\tau \leq \tau_{yw})$. In our model the amplitude ratio is represented by the complex modulus of the characteristic function, that we estimates as in Eq. (9) from simulations. Hence we search here for the threshold age, say it τ^* , for which the empirical young water fraction closely approximate the modulus of the empirical characteristic function.

We looked for the threshold age τ^* that minimizes the sum of squares of the distances between the modulus of the characteristic function and the young water fraction, as follows:

$$\tau^* = \operatorname{argmin}_{\tau_{yw}} \sum_{\alpha} (|\overline{H}_N| - F_{yw})^2, \quad (15)$$

where α ranges from 0.05 to 0.95 with step 0.01.

We performed the procedure for the 22 Swiss catchments, thus for different values of L , and we found τ^* between 46 and 76 days, as shown in Table 1, so in the range of 2.3 ± 0.8 months found by Kirchner (2016a) for a wide range of transit time distributions (von Freyberg et al., 2018). In addition, our results are in line with previous outcomes obtained by Gentile et al. (2023) who found a threshold age between about 44 and 96 days for the same catchments, but using a “direct input” approach for estimating the amplitude ratio of seasonal tracer cycles instead of the “delayed input” approach used by von Freyberg et al. (2018). For more details about “direct” and “delayed” input for estimating the amplitude ratio of seasonal tracer cycles the reader is referred to von Freyberg et al. (2018) and Gentile et al. (2023). The amplitude ratio A_s/A_p and the young water fraction F_{yw} are both dimensionless and they are both in the range from 0 to 1, so they can be directly compared to determinate the threshold age. Equivalently, the threshold age can be obtained with the fit between modulus of the characteristic function and young water fraction that minimizes the root mean squared error (RMSE) calculated relative to the 1:1 line. The threshold ages τ^* , reported in Table 1, were obtained with $RMSE \leq 0.01$. Plots for some of the 22 Swiss study catchments are shown in Fig. 4.

4.3. Passage time and heavy tail

The average transit time is infinite because the distribution of trapping Mittag-Leffler and therefore the distribution of transit time is heavy-tailed. Indeed, define the r.v. $\tau_L := \inf \{s \geq 0 : X(s) = L\}$. Note that

$$\tau_L = \frac{L}{v_0} \mathbb{1}_{[E_0 > \frac{L}{v_0}]} + (E_0 + J_0 + \tau'_L) \mathbb{1}_{[E_0 \leq \frac{L}{v_0}]} \geq J_0 \mathbb{1}_{[E_0 \leq \frac{L}{v_0}]}, \quad (16)$$

where τ'_L denote the amount of time after T_2 taken by X to reach the level L ; in formulae $\tau'_L \mathbb{1}_{[E_0 \leq \frac{L}{v_0}]} = \inf \{s \geq T_2 : X(s) = L\} - T_2$. Using (16) we get that

$$\mathbb{E}\tau_L \geq \mathbb{E}J_0 \mathbb{1}_{[E_0 \leq \frac{L}{v_0}]} = \mathbb{E}J_0 \mathbb{P}\left(E_0 \leq \frac{L}{v_0}\right) = +\infty \quad (17)$$

where we used independence of J_0 , v_0 and E_0 as well as the fact that J_0 has infinite expectation (since it has the Mittag-Leffler distribution). We observe that heavy tails for transit time distribution was already

observed (Wang et al., 2023; Kirchner, 2019; Porporato and Calabrese, 2015).

The infinite average transit time can also have an hydrologic interpretation. Indeed, the total catchment storage is composed of a mobile part (mobile aquifer groundwater connected with streamflow) and an “immobile” (the following clarifies why we use “”) part that does not participate in the catchment water fluxes (Staudinger et al., 2017). Accordingly, the infinite MTT suggests that an amount of water particles, through deep vertical infiltration, can reach portions of the subsurface (e.g., aquitard) that restrict the groundwater flow due to low permeability, thus confining deeper aquifers that are disconnected from watercourses. However, certain geological, hydrological and/or anthropic processes will, at some point, activate transverse dispersion from (extremely old) aquitard groundwater (likely constituting the “immobile” storage) to old (unconfined) aquifer groundwater (Torgersen et al., 2013) which is connected with watercourses. In such a case, the extremely old water particles would contribute to increasing the mean residence time in the aquifer that, sustaining baseflow during low-flow periods, will increase the streamwater MTT, thus also explaining the heavy tails of TTD. In this regard, radioactive tracers revealed that “fossil” (>12,000-year-old) groundwaters dominate global aquifer (about 250 m depth) storage (Jasechko et al., 2017), which can contribute to stream flow.

Another interpretation for mean transit times tending towards infinity can also be given by considering the water retained in a soil sample. It is known that, after sampling, the so-called “gravitational water” is lost, while the water that the soil retains against gravitational forces remains within it. Nevertheless, to quantify the gravimetric water content of a soil sample, the thermogravimetric method can be used, which involves drying the sample in an oven at 105 °C for at least 21 h so that even the water adsorbed by soil particles can evaporate. At ambient temperatures, this water does not participate in deep percolation and, if not taken up by plants, remains, for an indefinite time, in the soil held by the high negative tension. However, some processes (e.g., pedogenetic phenomena and/or the influence of soil fauna) could cause the soil to retain this water with less tension, which could then participate in gravitational flow, thereby increasing the average age of the percolating water (which is generally assumed to recharge groundwater). Although the aforementioned considerations lead us to find it acceptable to have a mean transit time tending towards infinity, the use of tracers does not help us to clearly validate this result and this is mainly for two reasons. First, tracers can help quantify the contribution of old vs. young streamflow but not *how old* the old water is (Knapp et al., 2019; Benettin et al., 2022). Second, a conceptual/mathematical model must be employed to convert tracer concentrations into an age and the model assumptions can have repercussions on the results (Torgersen et al., 2013). For example, by assuming a stationary TTD in the convolution integral approach, the stable-isotope-based MTT likely underestimates the true MTT, possibly by orders of magnitude (Kirchner, 2016a).

Although the mean transit time tends to infinite, order statistics, such as quantiles, i.e., the proportion of water younger than a threshold age (that we use in the next section to validate our model), are robust to the occurrence of extreme values. The asymptotic distribution can be often recognized explicitly, see for example, Chapter 10 in David and Nagaraja (2003) but also section 10.2 of Casella and Berger (2001).

4.4. Estimation of the trapping effect: the parameter α

In the proposed model for the movement of water particles in the subsurface we consider the Mittag-Leffler distribution for waiting times, whose parameter α is the only parameter of the model. As explained above, just after (6) and (7), this parameter is related to the length of waiting times, that is, the times in which the water particle does not move because it is trapped due to the heterogeneity of the catchment. The α parameter can be estimated by a polynomial fitting

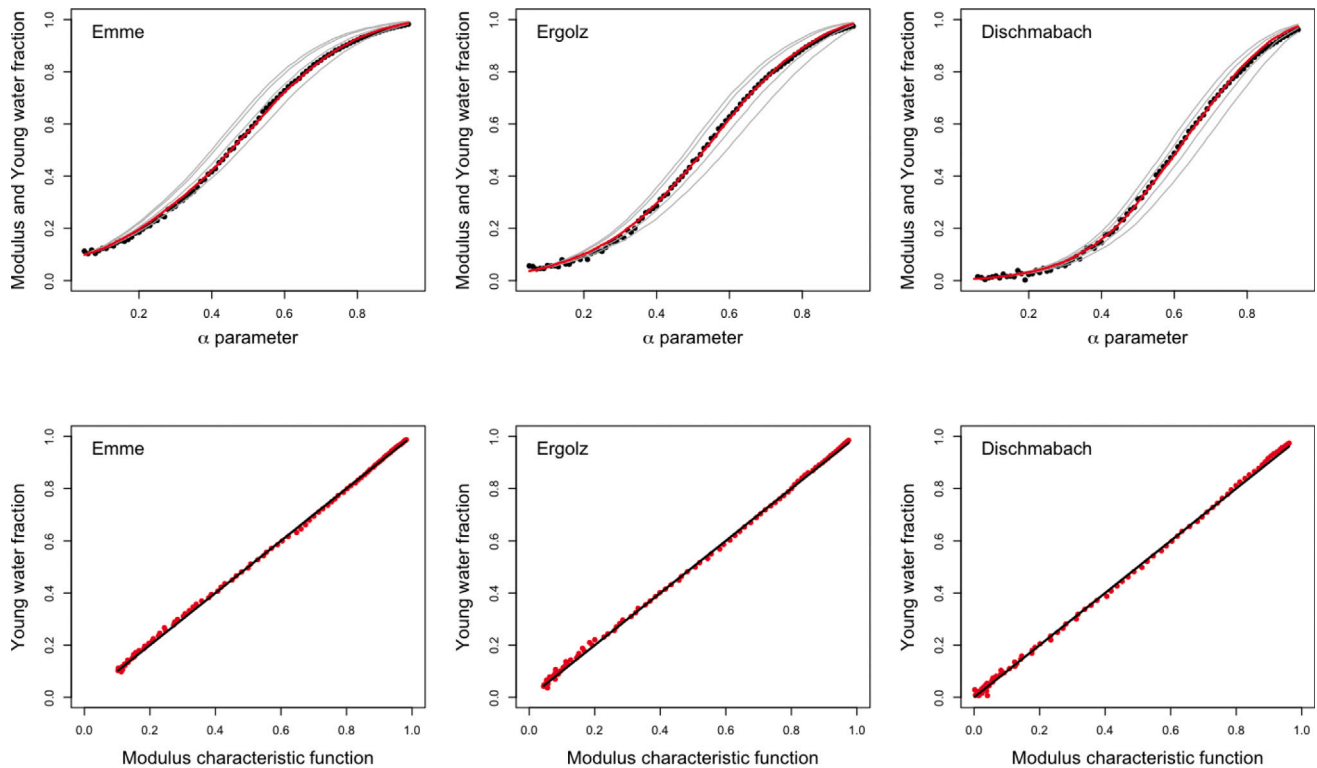


Fig. 4. In the top three plots the black points represent the modulus of the empirical characteristic function and the gray lines the young water fraction for different threshold ages. The best fits in red are obtained with threshold ages (τ^*) of 55, 63 and 76 days for catchments Emme, Ergolz and Dischmabach, respectively. The other three plots show in black the 1:1 line and in red the best fits with the same threshold ages for the three catchments.

of the modulus of the characteristic function which represents the empirical counterpart of the amplitude ratio of isotopic concentrations. The latter is observable, in the sense that it comes from a deterministic sinusoidal fitting of real data and its value for the 22 Swiss catchments is available from [Gentile et al. \(2023\)](#). The dependence between α and $|H(f)|$ should be estimated by fitting a suitable curve. We fitted the coefficients of polynomials with the mean square method and with a fourth order polynomial we obtain a $R^2 \approx 0.99$; see the curves in [Fig. 5](#) for some of the 22 Swiss study catchments.

Since the modulus of the characteristic function coincides with the ratio of the amplitudes of the isotopic concentrations, as stated in Section 2 (see Eq. (5)), by substituting the value of the amplitude ratio (A_s/A_p), reported in [Table 1](#), the fourth degree polynomial can be solved to estimate the value of α . The estimated values $\hat{\alpha}$, with a fourth-degree polynomial fitting, for each of the 22 Swiss study catchments are reported in [Table 1](#).

The amplitude ratio is related to the proportion of young water as follows. Small values of the amplitude ratio indicate that there is a lot of mixing within the catchment between incoming water (from precipitation and/or snowmelt) and groundwater storage that was previously present in the catchment (and, accordingly, it is older). As a result, the young water is low (e.g., the Dischmabach snow-dominated catchment, [von Freyberg et al. \(2018\)](#)). On the contrary, larger values of the amplitude ratio indicate a greater portion of young water (e.g., the Erlenbach hybrid catchment; [von Freyberg et al. \(2018\)](#) and [Gentile et al. \(2024\)](#)) due to limited mixing processes and the activation of rapid flow paths. In this sense, the alpha parameter is related to the mixing of young water with old water: a lower alpha value corresponds to longer traps (heavy tailed) and thus more mixing with water that was already stored in the catchment. This direct relation is well depicted

by our model as can be seen from the estimates of α ([Table 1](#)) and the trend of the modulus of the characteristic function, representing the amplitude ratio in our model, that increases from 0 to 1 with α ([Fig. 2](#)).

5. Discussion and conclusions

A probabilistic approach has already been introduced for anomalous (or non-Fickian) transport to describe tracer and water transport in heterogeneous systems. [Porporato and Calabrese \(2015\)](#) drew attention to existing theories of water age distributions and emphasized the importance of treating age distributions as random functions when hydrologic flows are modeled by means of time-varying stochastic processes. The introduction of stochasticity, originating from the randomness of the input and output terms in hydrological systems, can help improve streamflow models and quantify the uncertainty of water age. In addition, [Calabrese and Porporato \(2017\)](#) extended water age theory to multiple flows and analyzed the effects of nonlinearities.

On the other side Markovian mobile-immobile models and non-Markovian mobile-immobile models with heavy tails trapping time distribution for solute transport have been used ([Doerries et al., 2022](#); [Gao et al., 2010](#); [Schumer et al., 2003](#)), and also models based on continuous time random walks have been widely considered. Indeed a CTRW based on a power-law distribution of the transition times have been used to model the transport of a natural passive tracer (chloride) at a large spatial scale and over a long period ([Dentz et al., 2023](#)). Also, it was shown that CTRW model better describes the long tailed breakthrough curves of conservative tracers in an alpine karst system than the conventional advection–dispersion equation and the two-region non-equilibrium model, based on mobile and immobile

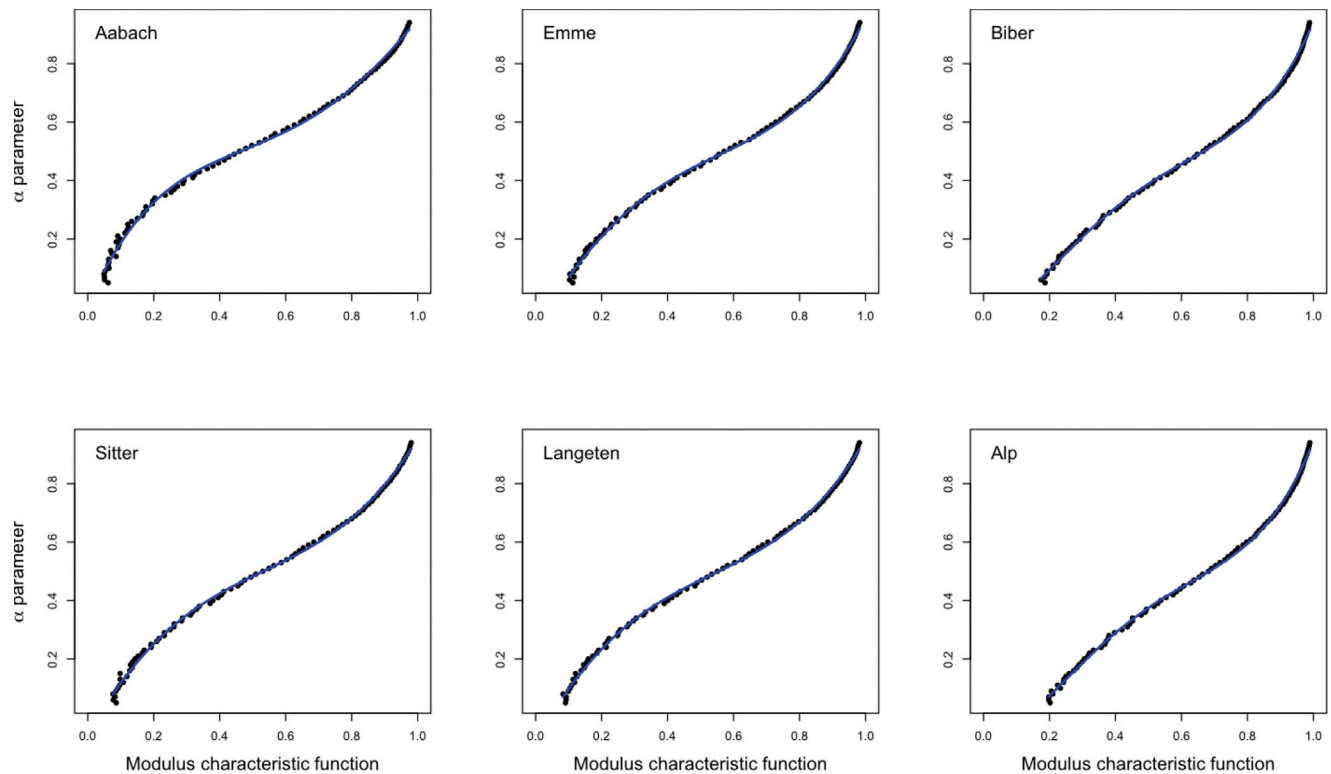


Fig. 5. Fourth degree polynomial fitting (in blue) over the modulus of the characteristic function to estimate the parameter α . These plots are relative to the catchments Aabach, Emme, Biber, Sitter, Langeten and Alp.

zones (Goepfert et al., 2020). An adaptation of the continuous time random walk-particle tracking model also to water flow in karst aquifers has been considered very recently (Elhanati et al., 2024) by simulating the contribution of fast and slow flow components.

Therefore the stochastic model we proposed, based on a random velocity process with rests, is new, in particular, in the context of subsurface water movement in heterogeneous catchments. This gave us the possibility to undertake several new considerations. The main strengths, and new features, of our model are the following. We make no explicit assumptions on the distribution of water transit time but make simple physical assumptions about the movement of water particles that take into account the heterogeneity of the subsurface. The only assumption is that the water particle alternates between periods in which it moves with constant velocity and periods in which it does not move (rests), so it has zero velocity, because it is trapped in the subsurface due to the heterogeneity of the catchment. We assume that moving times are i.i.d. random variables with exponential distribution, the waiting times are i.i.d. random variables with Mittag-Leffler distribution of order $\alpha \in (0, 1)$ and the velocities are i.i.d. random variables with uniform distribution in the interval $(1, 100)$. The distribution of trapping times (Mittag-Leffler) and thus the distribution of transit time is heavy-tailed, so the average transit time is infinite. We remark that not assuming a TTD is not necessarily an advantage, as other assumptions must be made upfront. However, it is more advantageous, conceptually, given that the TTD is generally a desired output.

The first passage time of the stochastic process through a certain level L , representing the transit time of water, is computed through simulations of the trajectories of millions of water particles. The median flow path length was chosen as level L because it is a representative measure for the length of the catchment, and thus we estimate the transit time distribution empirically. Furthermore, we determine that the complex modulus of the empirical transit time distribution coincides with the amplitude ratio of the isotopic concentrations in stream flow and precipitation. We observe that our approach is stationary, in the sense that we find only one TTD (for each catchment) which is based

on the model and the amplitude ratio that is a stationary input.

We applied the model to 22 Swiss catchments to estimate the young water fraction, i.e., the proportion of the empirical transit time distribution younger than a threshold age. Searching for the threshold age τ^* for which the young water fraction closely approximate the modulus of the empirical characteristic function, that in our model coincides with the amplitude ratio of isotopic concentrations, we found τ^* between 46 and 76 days, in agreement with the range of 2–3 months obtained previously in the literature (Kirchner, 2016a; Gentile et al., 2023).

Finally, it is possible to estimate the only model parameter, namely the α parameter of the Mittag-Leffler distribution, with a polynomial fitting of the modulus of the empirical characteristic function given the value of the amplitude ratio of the isotopic concentrations. The Mittag-Leffler distribution is the distribution chosen for waiting times so the α parameter is related to the length of trapping times in the sense that a lower value of alpha corresponds to longer traps, since the distribution is heavy-tailed, and thus to more mixing of young water with water that was already stored in the catchment. Therefore, lower values of alpha correspond to lower median flow path lengths or lower values of amplitude ratio of isotopic concentrations in stream flow and precipitation, i.e., to more mixing of young water with water that was already stored in the catchment.

Therefore, the main novelty of our paper is that we can argue that our model gives us information on the exit time of water from the catchment, in particular on the proportion of young water, and on the features of the motion inside the catchment. This agree with what is known in the literature and the model has only one parameter which is possible to estimate. In conclusion, random velocity processes with rests are a useful model for modeling subsurface water movement in heterogeneous catchments, and the validation of the model is done by using concentrations of stable water isotopes in precipitation and streamflows that are used to compute the young water fraction (Kirchner, 2016a,b).

CRedit authorship contribution statement

M.C. Bovier: Writing – review & editing, Writing – original draft, Conceptualization, Software, Methodology, Data curation, Formal analysis, Validation. **S. Fedotov:** Writing – review & editing, Supervision, Methodology, Validation, Conceptualization. **S. Ferraris:** Writing – review & editing, Supervision, Data curation, Conceptualization, Validation, Funding acquisition. **A. Gentile:** Writing – review & editing, Writing – original draft, Data curation, Validation, Conceptualization. **B. Toaldo:** Writing – review & editing, Supervision, Methodology, Conceptualization, Validation, Formal analysis, Funding acquisition.

Declaration of competing interest

The authors declare that they have no known competing financial interests or personal relationships that could have appeared to influence the work reported in this paper.

Acknowledgments

The authors A. Gentile and S. Ferraris have been supported by the project NODES, which has received funding from the MUR-M4C2 1.5 of PNRR with grant agreement no. ECS00000036, by the PRIN MIUR 2017SL7ABC 005 WATZON Project and by the PRIN 2022 202295PFKP SUNSET Project. The authors M.C. Bovier and B. Toaldo acknowledge financial support under the National Recovery and Resilience Plan (NRRP), Mission 4, Component 2, Investment 1.1, Call for tender No. 104 published on 2.2.2022 by the Italian Ministry of University and Research (MUR), funded by the European Union – NextGenerationEU – Project Title “Non-Markovian Dynamics and Non-local Equations” – 202277N5H9 - CUP: D53D23005670006 - Grant Assignment Decree No. 973 adopted on June 30, 2023, by the Italian Ministry of University and Research (MUR).

Appendix. Mathematical details

A.1. Amplitude ratio of seasonal isotope cycles

The equality (5) between the amplitude ratio of isotopic cycles in stream flow and precipitation and the complex modulus of the characteristic function can be ascertained as follows. By substituting the isotopes concentration (3) and (2) into the convolution Eq. (1), it follows that

$$A_s \sin(2\pi ft - \phi_s) + k_s = \int_0^\infty h(\tau)[A_p \sin(2\pi f\tau - \phi_p) + k_p]d\tau.$$

For the Euler’s formula the sine function can be written as $\sin x = \frac{e^{ix} - e^{-ix}}{2i}$, then

$$A_s \frac{e^{i2\pi ft} e^{-i\phi_s} - e^{-i2\pi ft} e^{i\phi_s}}{2i} + k_s = A_p \int_0^\infty h(\tau) \frac{e^{i2\pi f(\tau-t)} e^{-i\phi_p} - e^{-i2\pi f(\tau-t)} e^{i\phi_p}}{2i} d\tau + k_p$$

and thus

$$A_s(e^{i2\pi ft} e^{-i\phi_s} - e^{-i2\pi ft} e^{i\phi_s}) + 2i(k_s - k_p) = A_p[e^{i2\pi ft} e^{-i\phi_p} H(-f) - e^{-i2\pi ft} e^{i\phi_p} H(f)].$$

where we used the characteristic function (4).

Using the exponential of the logarithm and the complex logarithm $\log(H) = \log|H| + i\text{Arg}(H)$, where $\log|H(f)| = \log|H(-f)|$ and $\text{Arg}(H(-f)) = -\text{Arg}(H(f))$:

$$A_s(e^{i2\pi ft-i\phi_s} - e^{-i2\pi ft+i\phi_s}) + 2i(k_s - k_p) = A_p e^{\log|H|} [e^{i2\pi ft-i\phi_p-i\text{Arg}(H)} - e^{-i2\pi ft+i\phi_p+i\text{Arg}(H)}].$$

Using Euler’s formula $e^{ix} = \cos x + i \sin x$ and considering that cosine is an even function while sine is an odd function:

$$A_s \sin(2\pi ft - \phi_s) + (k_s - k_p) = A_p e^{\log|H|} \sin(2\pi ft - \phi_s - \text{Arg}(H)).$$

This equality is verified if

$$A_s = A_p e^{\log|H(f)|}, \quad \text{Arg}(H(f)) = \phi_s - \phi_p, \quad k_s = k_p,$$

so that

$$\frac{A_s}{A_p} = |H(f)|.$$

A.2. The random motion

Here is the precise mathematical formulation of the proposed model for the random motion. Let v_n , be a discrete time Markov chain on $[0, 100]$, with the transition probabilities on $[0, 100]$

$$p_v(dx) := P(v_{n+1} \in dx | v_n = v) = \begin{cases} \frac{dx}{99} \mathbb{1}_{[x \in (1,100)]}, & v = 0, \\ \delta_0(dx), & v \in (0, 100], \end{cases}$$

where $\delta_0(\cdot)$ represents the Dirac measure at zero and the initial distribution $\mu(dx)$ uniform on $(1, 100)$. Let $V(t)$ be a semi-Markov process on $[0, 100]$, representing the unit velocity vector of moving particle:

$$V(t) = v_n, \quad T_n \leq t < T_{n+1},$$

where T_n indicate the velocities switching times. The position of the particle is then obtained by integrating the velocity over time:

$$X(t) = \int_0^t V(\tau)d\tau, \quad t \geq 0.$$

The process $X(t)$ is as we described above, i.e., we have that

$$T_{n+1} - T_n = J_n \quad n = 1, 3, 5, 7, \dots$$

$$T_{n+1} - T_n = E_n \quad n = 0, 2, 4, 5, \dots$$

where J_n are the waiting times with Mittag-Leffler distribution and E_n are the moving times with exponential distribution.

The pair $(X(t), V(t))$ is a semi-Markov transport process, in the sense of Ricciuti and Toaldo (2023). In a semi-Markov transport process the evolution of a particle depends not only on the current state (position and velocity) but also on the time elapsed since the last change of velocity.

Data availability

Data will be made available on request.

References

Ali, K.F., De Boer, D.H., 2010. Spatially distributed erosion and sediment yield modeling in the upper indus river basin. *Water Resour. Res.* 46 (8), <http://dx.doi.org/10.1029/2009WR008762>, URL: <https://onlinelibrary.wiley.com/doi/abs/10.1029/2009WR008762>.

Baleanu, D., Diethelm, K., Trujillo, J.J., 2016. *Fractional Calculus Models and Numerical Methods*. In: *Series on Complexity, Nonlinearity and Chaos*.

Benettin, P., Bailey, S.W., Rinaldo, A., Likens, G.E., McGuire, K.J., Botter, G., 2017. Young runoff fractions control streamwater age and solute concentration dynamics. *Hydrol. Process.* 31 (16), 2982–2986. <http://dx.doi.org/10.1002/hyp.11243>, arXiv:<https://onlinelibrary.wiley.com/doi/pdf/10.1002/hyp.11243>. URL: <https://onlinelibrary.wiley.com/doi/abs/10.1002/hyp.11243>.

Benettin, P., Rodriguez, N.B., Sprenger, M., Kim, M., Klaus, J., Harman, C.J., van der Velde, Y., Hrachowitz, M., Botter, G., McGuire, K.J., Kirchner, J.W., Rinaldo, A., McDonnell, J.J., 2022. Transit time estimation in catchments: Recent developments and future directions. *Water Resour. Res.* 58 (11), e2022WR033096. <http://dx.doi.org/10.1029/2022WR033096>, URL: <https://agupubs.onlinelibrary.wiley.com/doi/abs/10.1029/2022WR033096>. e2022WR033096 2022WR033096.

Benson, D.A., Meerschaert, M.M., 2009. A simple and efficient random walk solution of multi-rate mobile/immobile mass transport equations. *Adv. Water Resour.* 32 (4), 532–539. <http://dx.doi.org/10.1016/j.advwatres.2009.01.002>, URL: <https://www.sciencedirect.com/science/article/pii/S0309170809000128>.

- Benson, D.A., Schmidt, M.J., Bolster, D., Harman, C., Engdahl, N.B., 2019. Aging and mixing as pseudo-chemical-reactions between, and on, particles: Perspectives on particle interaction and multi-modal ages in hillslopes and streams. *Adv. Water Resour.* 132, 103386. <http://dx.doi.org/10.1016/j.advwatres.2019.103386>, URL: <https://www.sciencedirect.com/science/article/pii/S0309170819303951>.
- Botter, G., Bertuzzo, E., Rinaldo, A., 2011. Catchment residence and travel time distributions: The master equation. *Geophys. Res. Lett.* 38 (11), <http://dx.doi.org/10.1029/2011GL047666>, arXiv:<https://agupubs.onlinelibrary.wiley.com/doi/pdf/10.1029/2011GL047666>. URL: <https://agupubs.onlinelibrary.wiley.com/doi/abs/10.1029/2011GL047666>.
- Calabrese, S., Porporato, A., 2017. Multiple outflows, spatial components, and nonlinearities in age theory. *Water Resour. Res.* 53 (1), 110–126. <http://dx.doi.org/10.1002/2016WR019227>, URL: <https://agupubs.onlinelibrary.wiley.com/doi/abs/10.1002/2016WR019227>.
- Casella, G., Berger, R., 2001. *Statistical Inference*. Duxbury Advanced Series.
- Cirpka, O.A., Fienen, M.N., Hofer, M., Hoehn, E., Tessarini, A., Kipfer, R., Kitandis, P.K., 2007. Analyzing bank filtration by deconvoluting time series of electric conductivity. *Groundwater* 45 (3), 318–328. <http://dx.doi.org/10.1111/j.1745-6584.2006.00293.x>, arXiv:<https://ngwa.onlinelibrary.wiley.com/doi/pdf/10.1111/j.1745-6584.2006.00293.x>. URL: <https://ngwa.onlinelibrary.wiley.com/doi/abs/10.1111/j.1745-6584.2006.00293.x>.
- David, H., Nagaraja, H.N., 2003. *Order Statistics*. Wiley.
- Dentz, M., Kirchner, J.W., Zehe, E., Berkowitz, B., 2023. The role of anomalous transport in long-term, stream water chemistry variability. *Geophys. Res. Lett.* 50 (14), e2023GL104207. <http://dx.doi.org/10.1029/2023GL104207>, arXiv:<https://agupubs.onlinelibrary.wiley.com/doi/pdf/10.1029/2023GL104207>. URL: <https://agupubs.onlinelibrary.wiley.com/doi/abs/10.1029/2023GL104207>. e2023GL104207 2023GL104207.
- Devlin, J., 2020. *Groundwater Velocity*. The Groundwater Project, Guelph, Ontario.
- Doerries, T.J., Chechkin, A.V., Schumer, R., Metzler, R., 2022. Erratum: Rate equations, spatial moments, and concentration profiles for mobile-immobile models with power-law and mixed waiting time distributions [phys. Rev. E 105, 014105 (2022)]. *Phys. Rev. E* 105, 029901. <http://dx.doi.org/10.1103/PhysRevE.105.029901>, URL: <https://link.aps.org/doi/10.1103/PhysRevE.105.029901>.
- Elhanati, D., Goepfert, N., Berkowitz, B., 2024. Karst aquifer discharge response to rainfall interpreted as anomalous transport. *Hydrol. Earth Syst. Sci. Discuss.* 2024, 1–25. <http://dx.doi.org/10.5194/hess-2024-46>, URL: <https://hess.copernicus.org/preprints/hess-2024-46/>.
- Freeman, T.G., 1991. Calculating catchment area with divergent flow based on a regular grid. *Comput. Geosci.* 17 (3), 413–422. [http://dx.doi.org/10.1016/0098-3004\(91\)90048-I](http://dx.doi.org/10.1016/0098-3004(91)90048-I), URL: <https://www.sciencedirect.com/science/article/pii/S009830049190048I>.
- Gao, G., Zhan, H., Feng, S., Fu, B., Ma, Y., Huang, G., 2010. A new mobile-immobile model for reactive solute transport with scale-dependent dispersion. *Water Resour. Res.* 46 (8), <http://dx.doi.org/10.1029/2009WR008707>, arXiv:<https://agupubs.onlinelibrary.wiley.com/doi/pdf/10.1029/2009WR008707>. URL: <https://agupubs.onlinelibrary.wiley.com/doi/abs/10.1029/2009WR008707>.
- Gentile, A., Canone, D., Ceperley, N., Gisolo, D., Previati, M., Zuecco, G., Schaeffli, B., Ferraris, S., 2023. Towards a conceptualization of the hydrological processes behind changes of young water fraction with elevation: a focus on mountainous alpine catchments. *Hydrol. Earth Syst. Sci.* 27 (12), 2301–2323. <http://dx.doi.org/10.5194/hess-27-2301-2023>, URL: <https://hess.copernicus.org/articles/27/2301/2023/>.
- Gentile, A., von Freyberg, J., Gisolo, D., Canone, D., Ferraris, S., 2024. Technical note: Two-component electrical-conductivity-based hydrograph separation employing an exponential mixing model (EXPECT) provides reliable high-temporal-resolution young water fraction estimates in three small Swiss catchments. *Hydrol. Earth Syst. Sci.* 28 (8), 1915–1934. <http://dx.doi.org/10.5194/hess-28-1915-2024>, URL: <https://hess.copernicus.org/articles/28/1915/2024/>. Publisher: Copernicus GmbH.
- Godec, A., Metzler, R., 2016. First passage time distribution in heterogeneity controlled kinetics: going beyond the mean first passage time. *Sci. Rep.* 6 (1), 20349. <http://dx.doi.org/10.1038/srep20349>, URL: <https://www.nature.com/articles/srep20349>.
- Goepfert, N., Goldscheider, N., Berkowitz, B., 2020. Experimental and modeling evidence of kilometer-scale anomalous tracer transport in an alpine karst aquifer. *Water Res.* 178, 115755. <http://dx.doi.org/10.1016/j.watres.2020.115755>, URL: <https://www.sciencedirect.com/science/article/pii/S004313542030292X>.
- Gooseff, M.N., Benson, D.A., Briggs, M.A., Weaver, M., Wollheim, W., Peterson, B., Hopkinson, C.S., 2011. Residence time distributions in surface transient storage zones in streams: Estimation via signal deconvolution. *Water Resour. Res.* 47 (5), <http://dx.doi.org/10.1029/2010WR009959>, arXiv:<https://agupubs.onlinelibrary.wiley.com/doi/pdf/10.1029/2010WR009959>. URL: <https://agupubs.onlinelibrary.wiley.com/doi/abs/10.1029/2010WR009959>.
- Jasechko, S., Perrone, D., Befus, K.M., Bayani Cardenas, M., Ferguson, G., Gleeson, T., Luijendijk, E., McDonnell, J.J., Taylor, R.G., Wada, Y., Kirchner, J.W., 2017. Global aquifers dominated by fossil groundwaters but wells vulnerable to modern contamination. *Nat. Geosci.* 10, 425–429. <http://dx.doi.org/10.1038/ngeo2943>.
- Kendall, C., McDonnell, J., 1998. *Isotope Tracers in Catchment Hydrology*. In: *Isotope Tracers in Catchment Hydrology*, Elsevier.
- Kirchner, J.W., 2003. A double paradox in catchment hydrology and geochemistry. *Hydrol. Process.* 17 (4), 871–874. <http://dx.doi.org/10.1002/hyp.5108>, URL: <https://onlinelibrary.wiley.com/doi/abs/10.1002/hyp.5108>.
- Kirchner, J., 2016a. Aggregation in environmental systems - part 1: Seasonal tracer cycles quantify young water fractions, but not mean transit times, in spatially heterogeneous catchments. *Hydrol. Earth Syst. Sci.* 20 (1), 279–297. <http://dx.doi.org/10.5194/hess-20-279-2016>, URL: <https://hess.copernicus.org/articles/20/279/2016/>.
- Kirchner, J., 2016b. Aggregation in environmental systems- part 2: Catchment mean transit times and young water fractions under hydrologic nonstationarity. *Hydrol. Earth Syst. Sci.* 20 (1), 299–328. <http://dx.doi.org/10.5194/hess-20-299-2016>, URL: <https://hess.copernicus.org/articles/20/299/2016/>.
- Kirchner, J.W., 2019. Quantifying new water fractions and transit time distributions using ensemble hydrograph separation: theory and benchmark tests. *Hydrol. Earth Syst. Sci.* 23 (1), 303–349. <http://dx.doi.org/10.5194/hess-23-303-2019>, URL: <https://hess.copernicus.org/articles/23/303/2019/>.
- Knapp, J.L.A., Neal, C., Schlumpf, A., Neal, M., Kirchner, J.W., 2019. New water fractions and transit time distributions at plynlimon, Wales, estimated from stable water isotopes in precipitation and streamflow. *Hydrol. Earth Syst. Sci.* 23 (10), 4367–4388. <http://dx.doi.org/10.5194/hess-23-4367-2019>, URL: <https://hess.copernicus.org/articles/23/4367/2019/>.
- Kurilovich, A.A., Mantsevich, V.N., Mardoukhi, Y., Stevenson, K.J., Chechkin, A.V., Palyulin, V.V., 2012. Non-Markovian diffusion of excitons in layered perovskites and transition metal dichalcogenides. *Phys. Chem. Chem. Phys.* 24, 13941–13950. <http://dx.doi.org/10.1039/D2CP00557C>.
- Mainardi, F., 2010. *Fractional Calculus and Waves in Linear Viscoelasticity*. Imperial College Press.
- McGuire, K.J., McDonnell, J.J., 2006. A review and evaluation of catchment transit time modeling. *J. Hydrol.* 330 (3), 543–563. <http://dx.doi.org/10.1016/j.jhydrol.2006.04.020>, URL: <https://www.sciencedirect.com/science/article/pii/S0022169406002150>.
- McGuire, K.J., McDonnell, J.J., Weiler, M., Kendall, C., McGlynn, B.L., Welker, J.M., Seibert, J., 2005. The role of topography on catchment-scale water residence time. *Water Resour. Res.* 41 (5), <http://dx.doi.org/10.1029/2004WR003657>, URL: <https://onlinelibrary.wiley.com/doi/abs/10.1029/2004WR003657>.
- Meerschaert, M.M., Sikorskii, A., 2012. *Stochastic Models for Fractional Calculus*. De Gruyter, Berlin, Boston, <http://dx.doi.org/10.1515/9783110258165>.
- Meerschaert, M.M., Toaldo, B., 2019. Relaxation patterns and semi-Markov dynamics. *Stochastic Process. Appl.* 129 (8), 2850–2879. <http://dx.doi.org/10.1016/j.spa.2018.08.004>, URL: <https://www.sciencedirect.com/science/article/pii/S0304414918304095>.
- Metzler, R., Klafter, J., 2000. The random walk's guide to anomalous diffusion: a fractional dynamics approach. *Phys. Rep.* 339 (1), 1–77. [http://dx.doi.org/10.1016/S0370-1573\(00\)00070-3](http://dx.doi.org/10.1016/S0370-1573(00)00070-3), URL: <https://www.sciencedirect.com/science/article/pii/S0370157300000703>.
- Nobre, A.D., Cuartas, L.A., Hodnett, M., Rennó, C.D., Rodrigues, G., Silveira, A., Waterloo, M., Saleska, S., 2011. Height above the nearest drainage – a hydrologically relevant new terrain model. *J. Hydrol.* 404 (1), 13–29. <http://dx.doi.org/10.1016/j.jhydrol.2011.03.051>, URL: <https://www.sciencedirect.com/science/article/pii/S0022169411002599>.
- O'Callaghan, J.F., Mark, D.M., 1984. The extraction of drainage networks from digital elevation data. *Comput. Vis. Graph. Image Process.* 28 (3), 323–344. [http://dx.doi.org/10.1016/S0734-189X\(84\)80011-0](http://dx.doi.org/10.1016/S0734-189X(84)80011-0), URL: <https://www.sciencedirect.com/science/article/pii/S0734189X84800110>.
- Payn, R.A., Gooseff, M.N., Benson, D.A., Cirpka, O.A., Zarnetske, J.P., Bowden, W.B., McNamara, J.P., Bradford, J.H., 2008. Comparison of instantaneous and constant-rate stream tracer experiments through non-parametric analysis of residence time distributions. *Water Resour. Res.* 44 (6), <http://dx.doi.org/10.1029/2007WR006274>, arXiv:<https://agupubs.onlinelibrary.wiley.com/doi/pdf/10.1029/2007WR006274>. URL: <https://agupubs.onlinelibrary.wiley.com/doi/abs/10.1029/2007WR006274>.
- Porporato, A., Calabrese, S., 2015. On the probabilistic structure of water age. *Water Resour. Res.* 51 (5), 3588–3600. <http://dx.doi.org/10.1002/2015WR017027>, URL: <https://agupubs.onlinelibrary.wiley.com/doi/abs/10.1002/2015WR017027>.
- Ricciuti, C., Toaldo, B., 2023. From semi-Markov random evolutions to scattering transport and superdiffusion. *Comm. Math. Phys.* 401, 2999–3042. <http://dx.doi.org/10.1007/s00220-023-04705-w>.
- Rigon, R., Banerji, M., Green, T.R., 2016. Age-ranked hydrological budgets and a travel time description of catchment hydrology. *Hydrol. Earth Syst. Sci.* 20 (12), 4929–4947. <http://dx.doi.org/10.5194/hess-20-4929-2016>, URL: <https://hess.copernicus.org/articles/20/4929/2016/>.
- Rinaldo, A., Benettin, P., Harman, C.J., Hrachowitz, M., McGuire, K.J., van der Velde, Y., Bertuzzo, E., Botter, G., 2015. Storage selection functions: A coherent framework for quantifying how catchments store and release water and solutes. *Water Resour. Res.* 51 (6), 4840–4847. <http://dx.doi.org/10.1002/2015WR017273>, arXiv:<https://agupubs.onlinelibrary.wiley.com/doi/pdf/10.1002/2015WR017273>. URL: <https://agupubs.onlinelibrary.wiley.com/doi/abs/10.1002/2015WR017273>.
- Scalas, E., 2006. Five years of continuous-time random walks in econophysics. In: *Namatame, A., Kaizouji, T., Aruka, Y. (Eds.), The Complex Networks of Economic Interactions*. Springer Berlin Heidelberg, pp. 3–16.

- Schumer, R., Benson, D.A., Meerschaert, M.M., Baeumer, B., 2003. Fractal mobile/immobile solute transport. *Water Resour. Res.* 39 (10), <http://dx.doi.org/10.1029/2003WR002141>, arXiv:<https://agupubs.onlinelibrary.wiley.com/doi/pdf/10.1029/2003WR002141>. URL: <https://agupubs.onlinelibrary.wiley.com/doi/abs/10.1029/2003WR002141>.
- Seeger, S., Weiler, M., 2014. Reevaluation of transit time distributions, mean transit times and their relation to catchment topography. *Hydrol. Earth Syst. Sci.* 18 (12), 4751–4771. <http://dx.doi.org/10.5194/hess-18-4751-2014>, URL: <https://hess.copernicus.org/articles/18/4751/2014/>.
- Somers, L.D., McKenzie, J.M., 2020. A review of groundwater in high mountain environments. *WIREs Water* 7 (6), e1475. <http://dx.doi.org/10.1002/wat2.1475>, URL: <https://onlinelibrary.wiley.com/doi/abs/10.1002/wat2.1475>.
- Staudinger, M., Stoelzle, M., Seeger, S., Seibert, J., Weiler, M., Stahl, K., 2017. Catchment water storage variation with elevation. *Hydrol. Process.* 31 (11), 2000–2015. <http://dx.doi.org/10.1002/hyp.11158>, URL: <https://onlinelibrary.wiley.com/doi/abs/10.1002/hyp.11158>.
- Tetzlaff, D., Seibert, J., Soulsby, C., 2009. Inter-catchment comparison to assess the influence of topography and soils on catchment transit times in a geomorphic province; the Cairngorm mountains, Scotland. *Hydrol. Process.* 23 (13), 1874–1886. <http://dx.doi.org/10.1002/hyp.7318>, URL: <https://onlinelibrary.wiley.com/doi/abs/10.1002/hyp.7318>.
- Torgersen, T., Purtschert, R., Phillips, F.M., Plummer, L.N., Sanford, W.E., Suckow, A., 2013. Defining groundwater age (chapter 3). In: *Isotope Methods for Dating Old Groundwater*. International Atomic Energy Agency (IAEA).
- von Freyberg, J., Allen, S., Seeger, S., Weiler, M., Kirchner, J., 2018. Sensitivity of young water fractions to hydro-climatic forcing and landscape properties across 22 swiss catchments. *Hydrol. Earth Syst. Sci.* 22 (7), 3841–3861. <http://dx.doi.org/10.5194/hess-22-3841-2018>, URL: <https://hess.copernicus.org/articles/22/3841/2018/>.
- Wang, S., Hrachowitz, M., Schoups, G., Stumpp, C., 2023. Stable water isotopes and tritium tracers tell the same tale: no evidence for underestimation of catchment transit times inferred by stable isotopes in StorAge selection (SAS)-function models. *Hydrol. Earth Syst. Sci.* 27 (16), 3083–3114. <http://dx.doi.org/10.5194/hess-27-3083-2023>, URL: <https://hess.copernicus.org/articles/27/3083/2023/>.
- Zaburdaev, V., Denisov, S., Klafter, J., 2015. Lévy walks. *Rev. Modern Phys.* 87, 483–530. <http://dx.doi.org/10.1103/RevModPhys.87.483>, URL: <https://link.aps.org/doi/10.1103/RevModPhys.87.483>.